NASA CR-135435
HRI-391

HIGH RESOLUTION MASKS FOR ION MILLING PORES THROUGH SUBSTRATES OF BIOLOGICAL INTEREST

by Sandra S. Donovan

HORIZONS RESEARCH INCORPORATED

prepared for

NATIONAL AERONAUTICS AND SPACE ADMINISTRATION

NASA-Lewis Research Center

Contract NAS3-21054

NASA CR-135435
HRI-391

HIGH RESOLUTION MASKS FOR ION MILLING PORES THROUGH SUBSTRATES OF BIOLOGICAL INTEREST

by Sandra S. Donovan

HORIZONS RESEARCH INCORPORATED

prepared for

NATIONAL AERONAUTICS AND SPACE ADMINISTRATION

NASA-Lewis Research Center

Contract NAS3-21054

TABLE OF CONTENTS

HIGH RESOLUTION MASKS FOR ION MILLING PORES THROUGH SUBSTRATES OF BIOLOGICAL INTEREST

1.0 SUMMARY

The purpose of the program was to investigate the feasibility of electrochemically oxidizing vapor deposited aluminum coatings to produce porous aluminum oxide coatings with submicron pore diameters and with straight channels normal to the substrate surface. The porous aluminum oxide coatings so produced would be used as integral sputter masks for ion beam etching the hole patterns through the underlying substrate. The ultimate goal is the development of an economical process for fabricating membranes with uniform submicron size pores for biomedical and other ultra filtration applications.

To this end, the substrates of stainless 304, copper, Teflon, and Kapton, as well as metallic aluminum were examined. Aluminum was vapor deposited on all of the non-aluminum substrates, and subsequently anodized.

The copper, stainless, and Kapton substrates were capable of taking the best vapor deposition. Even with water cooling and a thick Teflon sample, Teflon deformed during the vapor deposition process, yielding an unsatisfactory oxide with the exception of one sample.

During the program 58 samples were anodized, 19 were of sufficient quality to be delivered to NASA-Lewis, and 11 of these 19 were recommended for subsequent ion milling by NASA-Lewis. Of these 11 samples, 4 were on aluminum, 4 on copper, 2 on Kapton, and 1 on Teflon. The stainless would probably have worked well also if more stainless samples had been available.

In general, the channels of the oxide fabricated from the vapor deposited aluminum on copper and Kapton were straight, and superior to those fabricated on the Teflon and on the metallurgically worked aluminum metal. In all probability the Teflon would work as well if the vapor deposition process is refined to take into account Teflon's relative ease of deformation.

It is possible to produce an integral oxide-substrate structure with no or minimal intervening residual aluminum. To do this consistently, the procedures used in this exploratory program need refinement.

For those samples fabricated at 600 volts, the pore diameters were 0.4 to 0.6 micron, with center-to-center spacing of 0.7 to 0.8 micron. For those samples fabricated at 300 volts, the pore diameters were typically 0.3 micron with center-to-center spacing averaging about 0.4 micron.

The pore enlargement done on Sample N41 resulted in pore diameters as large as 0.9 micron.

Chemicals for the final cleanup of oxide from the substrates are discussed.

A simple conservative estimate of the needed direct labor and materials for preparing 25 micron thick vapor deposited aluminum coatings using a continuous wire fed 12 KW unit with intermetallic composite boats is anticipated to be $2 to $3 per square foot. To process this coating to an oxide mask, the direct labor and materials is anticipated to be about $2 to $3 per square foot. Thus the total direct labor and materials costs are anticipated to be $4 to $6 per square foot.

2.0 FABRICATION OF COATINGS

This section describes the substrates used, procedures to prepare substrates, and procedures to prepare and process the oxide coatings.

2.1 Preparation of Substrates

Substrates of interest to NASA-Lewis which were used in this program included aluminum, stainless steel, copper, Teflon and Kapton.

2.1.1 Aluminum Substrate

Aluminum was the first substrate prepared and anodized, as it was felt this would be the easiest substrate to control since it did not require vapor deposition.

The first aluminum sheet examined was commercially pure 1100, nominally 3.5 mils (0.0089 cm) thick. Early scanning electron microscope analysis showed this alloy to yield an unsuitable irregular structure, characterized by rough channel walls.

The next two aluminum alloys used were 99.999% aluminum and 99.99% aluminum. The latter was rolled at NASA-Lewis from an initial thickness of 20 mils (0.0508 cm) to 11.5 mils (0.0292 cm) when it was found that chemical thinning left too rough a surface. However, even 11.5 mils generally was too great for the program.

The 99.999% pure aluminum was also rolled at NASA-Lewis from an initial thickness of 10 mils (0.0254 cm) to nominally 3.7 mils (0.0094 cm), and was used extensively throughout the program. Since so much work had been put into the metal, grain growth and grain boundaries were apparent, which Horizons Research (HR) believed led to the stressed appearance of much of the porous oxide fabricated from it. This will be further discussed in Sections 3.2 and 4.0.

The nominal 3.7 mils thickness was selected on the following basis. Preliminary data from NASA-Lewis indicated that aluminum metal would ion mill about 3.5 times faster than the porous aluminum oxide. Since a final aluminum substrate thickness of 13 to as much as 50 microns was desired, an oxide thickness of 4 to 14 microns would be needed for the mask. However, to fabricate a final oxide in these thickness ranges, as much as 40 microns of oxide grown at low voltages had to be fabricated and chemically removed, allowing an extra 3 microns for leeway. To fabricate an oxide thickness of 14 + 40 + 3 microns, and having determined that a given thickness of this aluminum will produce an oxide 122% on the average thicker than the metal, it was calculated that 57/1.22 or 47 microns of aluminum, at most, would be needed. Adding this value to the maximum 50 microns of aluminum substrate desired, the result is 97 microns or about 3.8 mils.

For the thin 13 micron substrate, it would have been desirable to have a sheet of starting aluminum thinner than 3.7 mils, but such was not possible at the time. For this 13 micron substrate, the resultant oxide was thicker than necessary.

2.1.2 Stainless Steel Substrate

On the 1/2 mil, 304 stainless steel substrates, coated with a 1 to 2 microns of ion beam sputter deposited aluminum by NASA-Lewis, Horizons Research vapor deposited an additional 3.2 mils (80 microns). The rationale for this thickness was as follows. Stainless ion mills about 1.6 times faster than the porous aluminum oxide. A 13 micron stainless substrate would require 21 microns of oxide mask. It was not known if the 122% expansion factor would be present in a vapor deposited metal so no adjustment was made for it. It was felt that about 40 microns of low voltage oxide would be needed, and for these initial runs an extra 19 microns should be added as a safety factor; hence, 21 + 40 + 19 = 80 microns. No special problems were encountered in vapor depositing aluminum onto the stainless.

2.1.3 Copper Substrate

Halfway through the program, 0.6 mil copper was substituted for the stainless. The copper was coated with an ion beam sputter deposited 1 to 2 micron thick layer of aluminum by NASA-Lewis. Horizons Research generally added an additional 25 microns of vapor deposited aluminum, having learned from the results with the stainless steel that 80 microns were not needed, and having been requested by NASA-Lewis to minimize oxide thickness even at the expense of some decrease in pore size or spacing. Copper ion mills six times faster than the oxide. Thus, a 13 micron thick copper membrane would need only 2 microns of oxide, but generally more would have to be left on for a safety margin. Copper did not present any vapor deposition difficulties.

2.1.4 Teflon Substrate

A severe problem was encountered during the vapor deposition of aluminum onto the one-half mil and one mil thick Teflon substrates. As with the stainless steel and copper substrates, the Teflon had been previously coated with 1 to 2 microns of ion beam sputter deposited aluminum. Heat from the evaporation source caused extreme wrinkling and distortion problems during vapor deposition, even after a water cooled jacket was added behind the Teflon target. One mil thick Teflon produced only one deliverable specimen, N-48.

A thicker Teflon substrate of 58.5 mils (0.149 cm) was tried for 2 runs. In both cases, the Teflon deformed during vapor deposition, causing cracks in the vapor deposited aluminum and unsatisfactory oxide growth.

2.1.5 Kapton Substrate

Kapton, 0.6 mil thick, also coated with 1 to 2 microns of ion beam sputter aluminum deposited by NASA-Lewis, offered no special vapor deposition problems once the water cooled jacket behind the target was added. Kapton mills about 1.4 times faster than the oxide, so generally 25 to 30 microns of additional vapor deposited aluminum were added.

2.2 Fabrication of Oxide Coating

This subsection discusses in turn the formation of the oxide, the removal of the unwanted low voltage oxide, pore enlargement, and final substrate cleanup.

2.2.1 Formation of Oxide

Electrochemical oxidation of aluminum metal under controlled conditions (see Appendix I for technical review) will form an oxide with parallel channels extending through its thickness. These channels are open at one end and capped at the other by a removable, extremely thin, continuous oxide layer called the barrier layer.

Figure 1 shows the oxide's structure. The pore diameter is a function of voltage, electrolyte type, electrolyte concentration and temperature. Center-to-center spacing of the pores is primarily a function of voltage. When electrochemically fabricated, the oxide is in the gamma form.

The aluminum oxide was fabricated in 4.5 cm diameter discs, on approximately 6 cm x 6 cm substrates, from vapor deposited or metallic aluminum in an oxalic acid electrolyte. The fabrication cell is shown in Figure 2. In operation, the cell is tilted so that the electrolyte covers the specimen even with the circulation pumps off. The pumps deliver fresh, cooled electrolyte to the face of the oxide specimen at the rate of 600 gph, and cooled glycol to the back aluminum side of the specimen

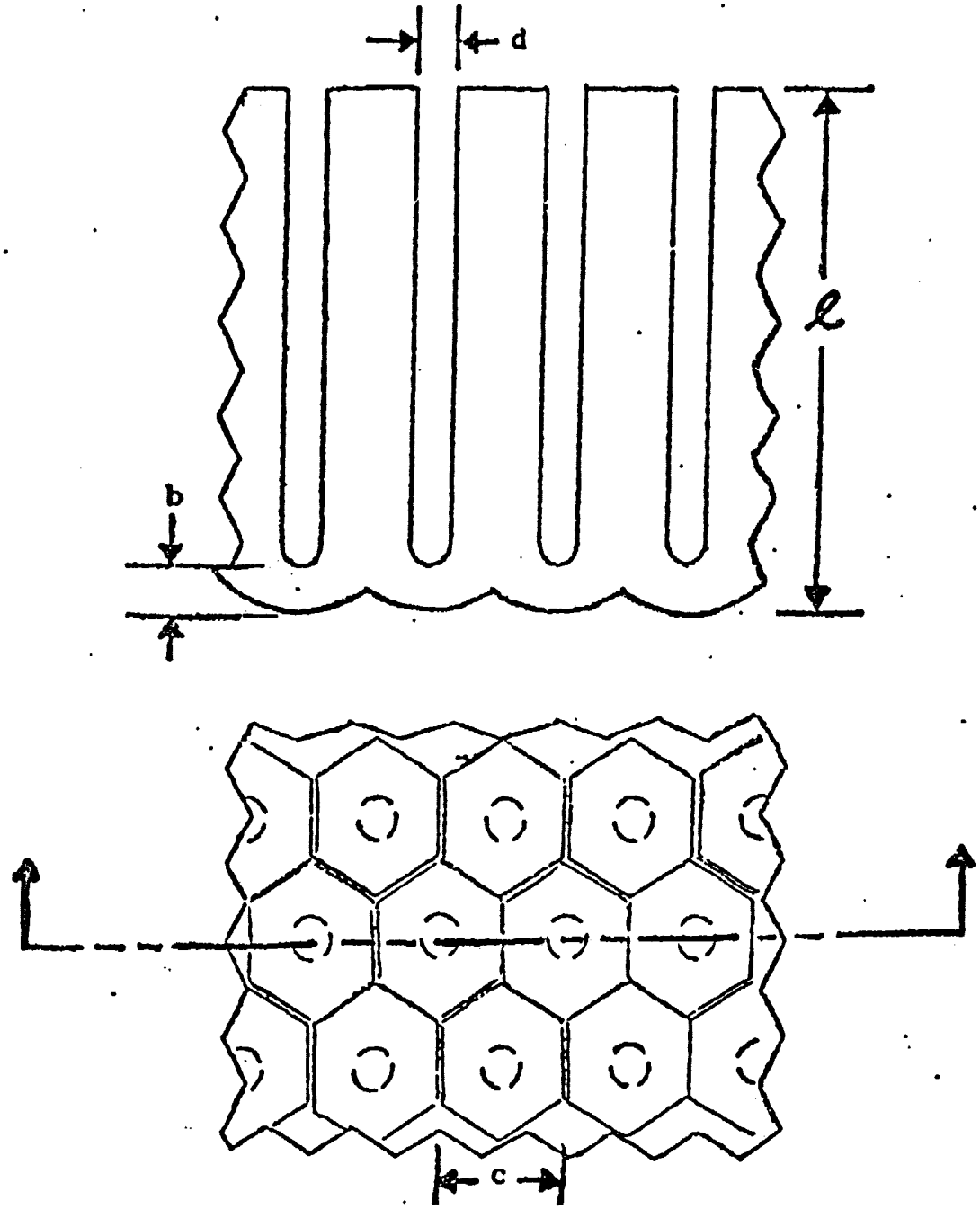

Figure 1. Porous aluminum oxide geometry. (Showing the oxide thickness of channel length ℓ, pore diameter d, barrier layer thickness b, and cell size c)

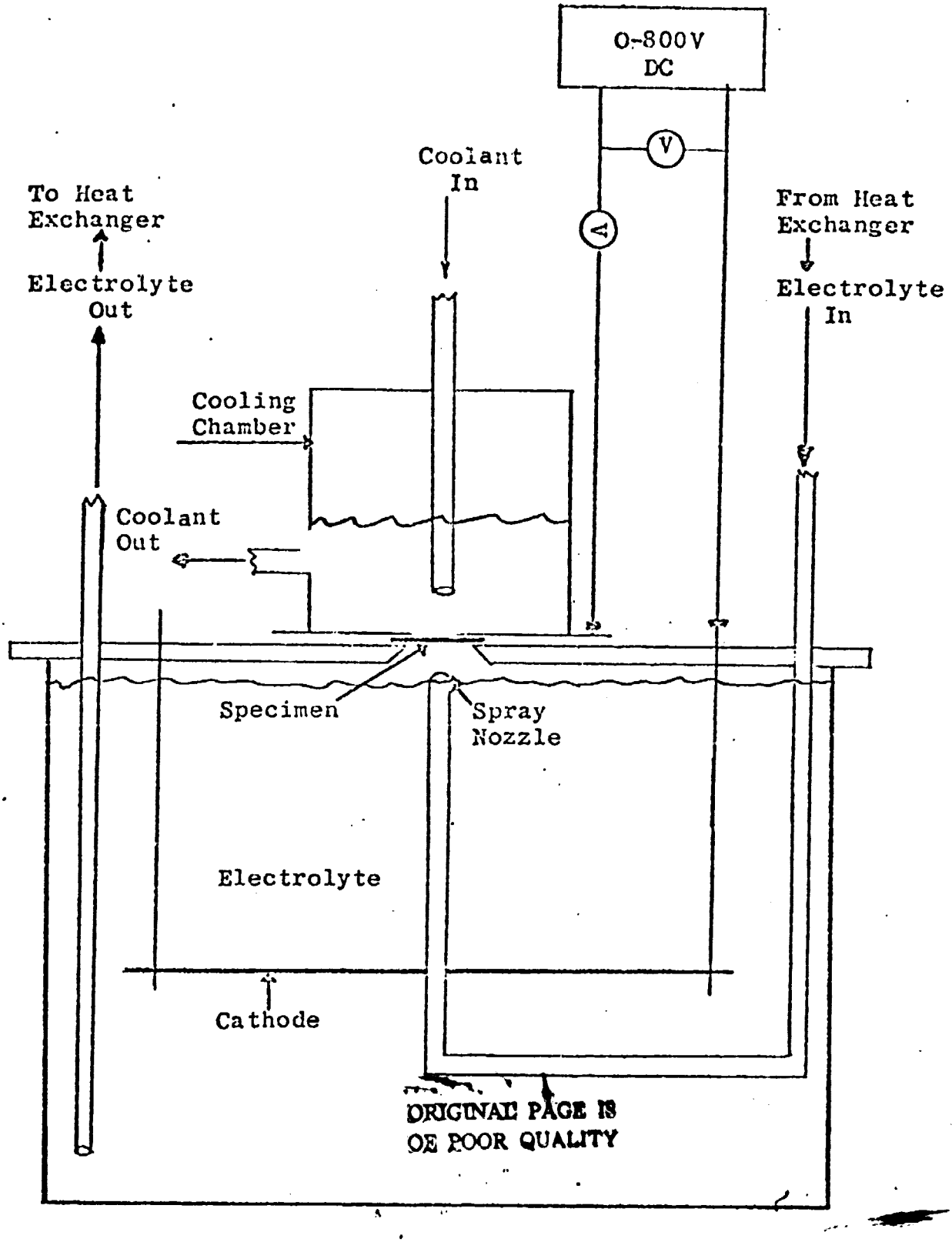

Figure 2. High Voltage Anodizing Cell

at the rate of 350 gph. The 1/2 ton heat exchanger is capable of maintaining electrolyte temperature to within 0.5°C at 2°C when both fabrication cells are in operation. The equipment is capable of providing up to 800 volts DC, with appropriate current, voltage, and temperature monitoring. Final voltages of 200 to 600 volts were used.

On a number of substrate samples, especially the aluminum metal ones, a precoat of oxide was put on prior to the anodizing. This precoat was typically 9 microns thick and formed at low voltages and high current densities. It has been found effective as an aid to reaching high voltages without building up excessively thick low voltage sections.

For about half of the program, when a maximum of 600 volts was reached, two fabrication electrolytes were used. The first electrolyte permitted a rapid increase in voltage to the desired 600 volts, resulting in a minimum amount of the unwanted intermediary oxide growth which would be removed chemically prior to ion milling. The second electrolyte permitted rapid growth at the desired constant high voltage.

The first electrolyte was an aqueous solution containing 1% or 0.5% oxalic acid and 0.1% titanium IV oxalate, $K_2TiO(C_2O_4)\cdot 2H_2O$. Generally, the 1% oxalic acid solution was too strong. The second electrolyte was a 5% or a 2% oxalic acid aqueous solution. The 2% solution was generally more satisfactory. For both the solutions, the electrolyte temperature was about 25°C. With these conditions, the initially grown intermediary oxide which was removed chemically was 20 to 40 microns thick, the pore diameter of the 600 volt oxide section 0.4 to 0.6 microns, and the center-to-center spacing generally 0.7 to 0.8 microns.

The mode of operation for using these two solutions was as follows:

1. Fabrication of the oxide in an aqueous solution containing 1% or 0.5% oxalic acid and 0.1 titanium (IV) salt while the voltage is being increased from 0 to 600 volts.

2. Power turned off.

3. Titanium containing solution pumped out of cell; cell and lines rinsed with deionized water.

4. 5% or 2% Oxalic acid solution pumped into cell.

5. Power turned on an desired high voltage section grown.

6. Power turned off, sample removed, and new sample put on.

7. 5% or 2% Oxalic acid solution pumped out, cell and lines rinsed with deionized water, and titanium containing solution returned to cell for a new run.

For the other half of the program a maximum of generally 300 volts was used, and only one anodizing solution was needed. This was an aqueous solution containing 0.25% oxalic acid and 0.1% titanium IV oxalate, $K_2TiO(C_2O_4)_2 \cdot 2H_2O$. Unwanted low voltage oxide thickness was typically 25 microns, with pore/diameters typically 0.3 micron, and center-to-center pore spacing typically near 0.4 micron.

2.2.2 Removal of Unwanted Oxide

The removal of the originally formed oxide at intermediary voltages was accomplished by pouring a chemical etchant, an aqueous nitric acid-hydrofluoric acid solution across the oxide surface. This etchant can be conveniently obtained as a commercial aluminum surface cleaner called Arcal Alum-Surf-Prep from Arcal Chemicals, Inc., 7320 86th Avenue, Seat Pleasant, MD 20027 (301/336-9300).

The specimen to be thinned was placed on an open woven screen, and the etchant (used full strength) slowly poured over the specimen and screen for typically 10 to 90 seconds, with occasional excursions to 3 minutes. The duration of the pour was determined from preliminary trials with small pieces of the sample to be thinned or with identical test samples. Generally two or three thinnings would be needed to remove the excess oxide to achieve the desired thickness. Care was taken not to remove excessive amounts. After each etchant treatment, the

sample was thoroughly rinsed with tap water.

Amounts of oxide removed were verified by optical microscope examination, and crosschecked by precision micrometers. The amount of oxide to be removed was determined by calculating the thickness of the low voltage section, knowing the number of coulombs passed, and continually verifying the electrochemical oxide formation efficiency by comparing measured and calculated oxide thicknesses. For high purity aluminum metal, under the anodizing conditions used here, the formation efficiency is virtually 100%. For the vapor deposited aluminum, the efficiency varied from 55 to virtually 100%, with generally the better products running near 100% efficiency.

For the sample size of 15.9 cm^2, the relationship between measured cell output and oxide thickness is

$$\underset{(\text{microns})}{\text{thickness}} = 150 \quad \underset{(\text{ampere})}{(\text{current})} \; \underset{(\text{hours})}{(\text{time})} \quad E$$

where E = efficiency. If the efficiency is 100%, E = 1.0. Thus 1 A passed for 1 hour at 100% efficiency would produce an oxide 150 microns thick. While increasing the voltage to the desired maximum, currents were typically around 0.3 to 0.6 A. At the maximum voltage, currents were more typically 10 to 30 mA.

2.2.3 Pore Enlargement

Pore enlargement was performed on only those samples which had 500 volts or 600 volts as their maximum voltage. The pore enlargement was done with a 2.5% water solution of Arcal. The dry specimen to be pore enlarged (still attached to its substrate), along with sufficient solution to cover it was placed in a small Pyrex container which was put into a mild ultrasonic cleaning unit (Cole-Parmer Model 8845-3). Typical residence time was 6 minutes.

Pore enlargement after ion milling was not done because ion milled samples were not yet available at the time of this report.

2.2.4 Final Removal of Oxide Coating from Substrates

For removal of excess oxide from an aluminum substrate, the Arcal solution at room temperature or

probably any (preferably non-etching or mildly etching) aluminum metal cleaner can be used.

For removal of excess oxide from a copper substrate, a 5 to 10% sodium hydroxide solution at room temperature will work. Such a solution attacks copper at the rate of less than 2 mils/year.

For removal of excess oxide from both stainless steel and Teflon, nitric acid can be used. A 10 to 20% room temperature solution should be adequate. Stainless steel Type 304 is attacked at the rate of less than 2 mils per year by this acid. Teflon has excellent resistance to acids.

For removal of excess oxide from Kapton, any dilute acid (~10%) solution at room temperature should be sufficient to dissolve the oxide and leave the Kapton unaffected.

After any of the above described treatments are performed, the substrate should be extremely well rinsed in water to remove any traces of the attacking chemical.

3.0 TECHNICAL DATA

Data obtained throughout this program are summarized in this section.

3.1 Anodizing Data

Table I summarizes the anodizing data. The thickness for the low voltage section does not include the precoat. thickness. If no value is given the precoat thickness column, then no precoat was present. For the final runs (N45-N58), 100% efficiency was assumed in calculating the thicknesses although subsequent Scanning Electron Microscope (SEM) examination showed that some had lower efficiencies. Generally the good specimens had 100% efficiency.

TABLE I

ANODIZING DATA

Run	Substrate	Anodizing Solution	V_{max} (volts)	Measured Thickness (μ)		
				Oxide	Metal	Precoat
N1	A	A	600	42		8
N2	A	A	596	15		9
3	A	A	604	24		--
N4	B	A,B	600	60		15
N5	B	A,B	600	--		15
N6	A	A	600	--		7
N7	A	A	550	--		7
N8	A	A	550	--		7
N9	A	A,B	550	55		7
N10	A	A,D	550	33	65	8
N11	A	A,D	550	50	57	7
N12	A	A,D	550	--		7
N13	A	A,D	550	--		7
N14	A	A	---	--		7
N15	A	A,D	550	--		7
N16	S	A	259	--		--
N17	S	A	521	40		--
N18	S	A	195	--		--
N19	C	A	500	--		--
N20	C	A	500	119		--
N21	K	A	192	17	40	--
N22	K	A	189	25	30	--
N23	C	A	500	150?	150?	--
N24	C	A,B	600	--		9
N25	C	A,B	600	--		9
N26	C	A,B	600	--		9
N27	D	A,B	600	75	33	9

Substrate Code: A = 1100 aluminum (3.7 mils)
B = 1199 aluminum (20 mils)
C = 1199 aluminum (11.5 mils)
D = 5-9's aluminum (3.7 mils)
S = Steel; T = Teflon
K = Kapton
Cu = Copper

Calculated Thickness		Efficiency	Anodizing Characteristics
Low V (μ)	High V (μ)		
143	---	24	Sparked
71	---	21	"
112	---	21	"
46.8	---	100	Fair to good
47.5	38.1	100	Fair to good
---	---	--	Bad
---	---	--	"
---	---	--	"
26	22	17.2	Good
25	---	31	Sparked
18	31	17.2	Good
38	---	17.2	Sparked
---	---	--	Bad
---	---	--	"
---	---	--	"
---	---	--	"
48.7	---	82	Bad edge
---	---	--	Bad
---	---	--	Too slow
142	---	84	" "
30.5	---	56	Bad edge
39.8	---	63	" "
---	---	--	Poor
92	15	100	Fair
---	---	--	Bad
66.6	77.8	100	Pitted
68.7	---	100	Fair

Anodizing Solution Code:
A = 1% oxalic + 0.1% Ti (V)
B = 5% oxalic
C = 0.5% oxalic + 0.1% Ti (V)
D = 2% oxalic
E = 0.25% oxalic + 0.1% Ti (V)

TABLE I (Cont'd.)

ANODIZING DATA

Run	Substrate	Anodizing Solution	V_{max} (volts)	Measured Thickness (μ) Oxide	Metal	Precoat
N28	D	A	484	--	--	--
N29	D	A,B	600	75	30	9
N30	D	C,D	600	~100	10	9
N31	D	C,B	469	--	--	9
N32	D	C	460	--	--	9
N33	D	C,D	600	~ 100	10	9
N34	D	C,D	600	~104	4	9
N35	D	C,D	600	70	6-10	9
N36	D	C,D	600	124	?	9
N37	D	C,D	600	--	--	9
N38	K	B	503	~ 15	~100	--
N39	K	B	506	--	--	--
N40	T	B	483	--	--	--
N41	D	C,D	600	18	--	9
N42	D	C,D	600	--	--	9
N43	C	C,B	600	--	--	9
N44	C	C,D	600	140-145	--	9
N45	S	E	300	36	N	--
N46	Cu	E	300	22 max.	N	--
N47	Cu	E	300	--	N	--
N48	T	E	200	10 max.	N	--
N49	Cu	E	300	13-14	N	--
N50	Cu	E	300	36	N	--
N51	Cu	E	300	--	N	--
N52	Cu	E	300	22	N	--
N53	Cu	E	300	--	N	--
N54	Cu	E	300	--	N	--
N55	K	E	290	--	N	--
N56	K	E	300	--	N	--
N57	T	E	195	--	--	--
N58	T	E	200	--	--	--

N = Some sections have none

Caculated Thickness		Efficiency	Anodizing Characteristics
Low V (μ)	High V (μ)		
---	---	--	Burned
67	---	100	"
38	40	100	Good
---	---	--	Burned
---	---	--	"
27.3	33	100	Good
29	52.1	100	"
28.9	39	100	"
28.8	32.6	100	"
16.5	36.3	100	"
11	---	100	Fair
17.9	---	100	"
---	---	--	Bad
10.6	21.8	100	Good
16.5	21.8	100	"
---	---	100	Bad
52.5	145	100	Good
11.3	56.4	(100)	Good
31.2	2.6	(100)	Fair
35.9	14.6	(100)	Good
20.8	6.1	(100)	"
22	15.9	(100)	"
22.4	78.4	(100)	"
22.2	8.5	(100)	"
21	11	(100)	"
32.5	17.9	(100)	"
28	28.8	(100)	"
26.2	21.6	(100)	"
26.5	18.2	(100)	"
19.5	---	(100)	Bad
15.3	6.4	(100)	"

TABLE II

SEM ANALYSIS

Run	Treatment	Thickness		Comments
		Oxide (μ)	Total (μ)	
N9	S	--	--	Knobby
N11	S	--	--	Knobby
N30	LVR	25-50	66	Curved channels; rough.
N33	LVR	20-40	71	Some curved channels.
N34	LVR	35-70	80	Some channels curved; rougher.
N35	LVR	25-50	70	Curved channels.
N36	LVR	25-35	85	Straight channels; some branching.
N37	PE+LVR	--	--	Too irregular.
N41(PE)R	PE+LVR	18	82	Not curved; some branching.
N41(PE)2	PE+LVR	18	82	Not curved; some branching.
N42	LVR	--	--	Treatment too severe.
N44	LVR	140-145	292	Wavy channels.
N45	LVR	36	94	Channels fairly straight; some rubble.
N46	LVR	22 max.	38	Straight channels.
N48	LVR	10 max.	43	Straight channels.
N49	LVR	13-14	51	Straight channels.
N50	LVR	36	41	Straight channels.
N52	LVR	13 + 9*	38	Straight channels.
N55	LVR	28	39	Straight channels.
N56	LVR	46	56	Straight channels.
N58	---	8.9 + 11.6	Thick	Straight channels, and gaps between layers.

*Some low voltage

Treatment Code: S = Stripped
LVR = low voltage removal
PE = pore enlargement

	Pore Size (μ)	Spacing (μ)	Conclusion
	--	--	1100 alloy unsuitable.
	--	--	" " "
	0.5	0.7	Poor.
	0.4-0.6	0.7	Do ion milling.
	0.5	0.7	Poor.
	0.6	~1	Poor.
	0.55	~0.8	Do ion milling.
	--	--	--
	0.8 on El. side 0.4-0.7 on B.L	~0.8	Do ion milling.
	0.8-0.9 on El. side 0.4-0.7 on B.L.	~0.8	Do ion milling.
	--	--	--
	--	--	Poor.
	Small	~0.8	Poor.
	0.3	~0.5	Do ion milling.
	0.1-0.2	0.2-0.3	Do ion milling.
	0.3	0.3-0.5	Do ion milling.
	0.3-0.4	~0.4	Do ion milling.
	0.3	~0.5	Do ion milling.
	0.4	0.5	Do ion milling.
	0.35-0.4	0.4	Do ion milling.
	--	--	Poor

3.2 SEM Analysis Data

Table II gives the SEM analysis data, along with a conclusion of sample quality. Note that N41(PE)R and N41(PE)2 are two halves of the same sample.

Reproductions of SEM photomicrographs of representative porous oxide coatings on aluminum, copper and Kapton substrates are shown in Figures 3 through 5, respectively. NASA-Lewis' Technical Monitor has glossy copies of all photomicrographs taken during the program.

Note that, in general, the oxides grown from vapor deposited aluminum on substrates that could tolerate the heat of the vapor deposition process had better structural uniformity than those oxides grown on the worked aluminum metal.

3.3 Delivered Samples

Table III lists delivered samples and suggested ion milling candidates and their quality.

3.4 Cost of Manufacturing Oxide Masks

Without becoming involved in a detailed cost analysis, and the capital equipment and overhead costs, it can be stated that the manufacturing costs for these masks are not prohibitive provided the vapor deposition can be done as described in the following paragraph.

If batch vapor deposition using tungsten helix coils is used, the cost of direct labor and materials to prepare 1 square foot of aluminum 25 microns thick is very high -- $70 to $120. However, if a continuous wire fed process using a 12 KW unit and Union Carbide's intermetallic composite boats is used, the cost of materials and direct labor is substantially reduced to $2 to $3 per square foot for a 25 micron thick coating. This estimate is based on information primarily received from Mr. M. A. Roache of Union Carbide Corp. (216/433-8600, Ext. 716).

The direct labor and materials cost for converting the aluminum coating to an oxide mask is estimated conservatively at $2 to $3 per square foot.

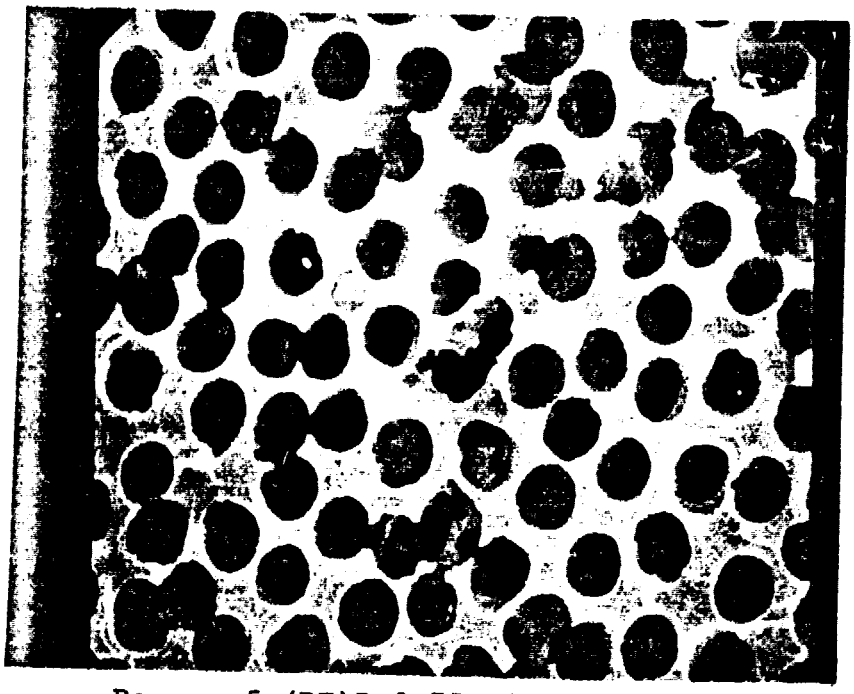

Pores of (PE)R 0.75 micron diameter
(10,000X)

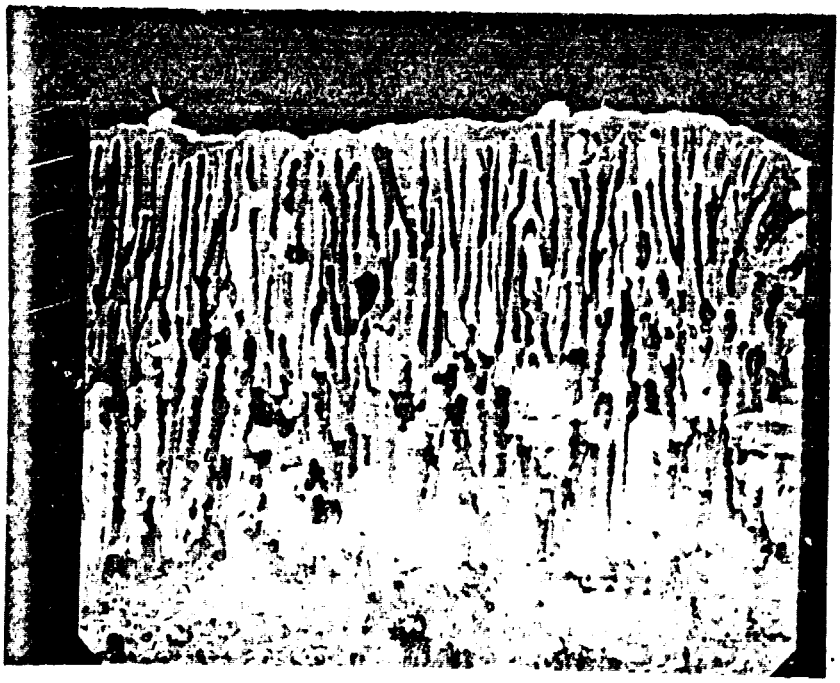

Channels of N-41 (PE)2
(3,000X)

Figure 3. Sample N-41, Aluminum Substrate, 600 Volts Max., Pore Enlargement Done.

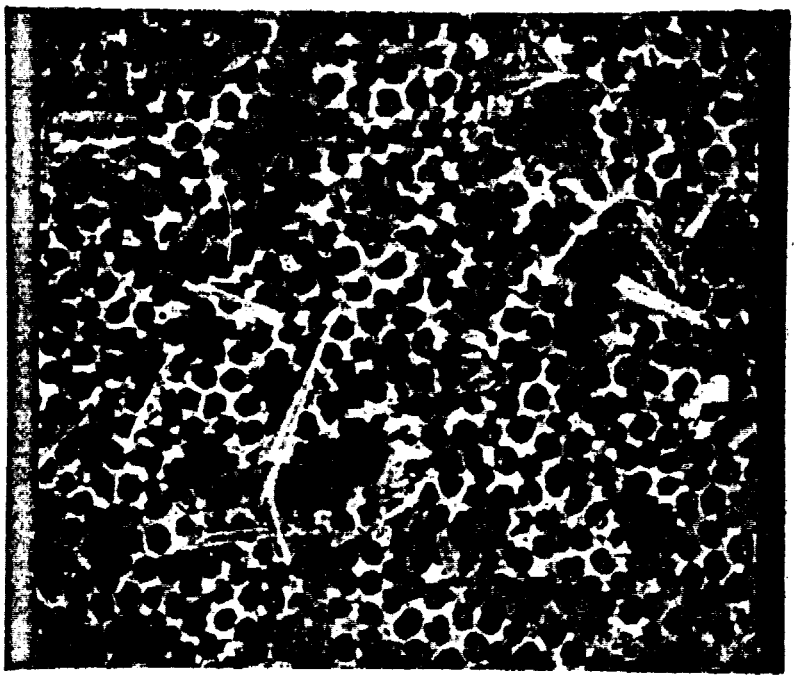

Pores,0.35 micron diameter
(10,000X)

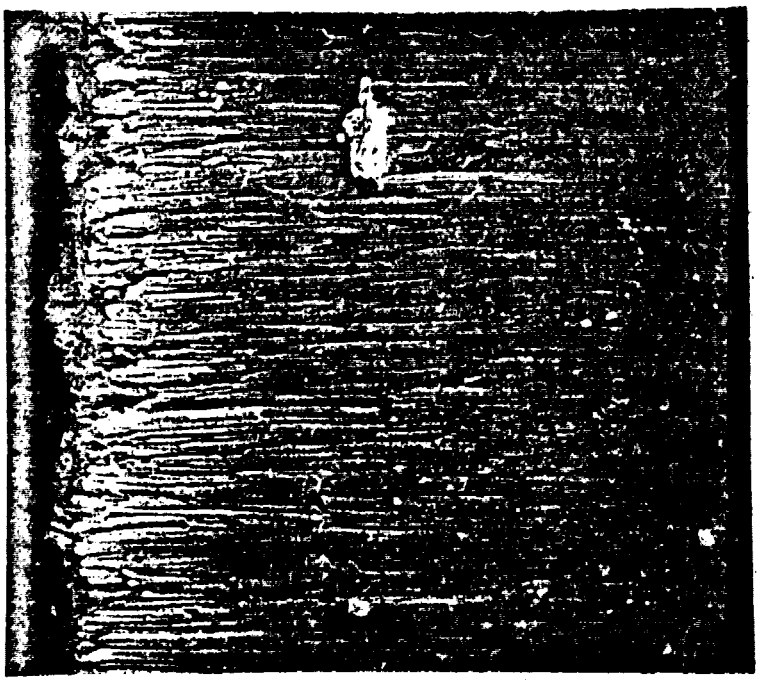

Channels, 36 microns of oxide thickness
(3,000X) (not all shown).

Figure 4. Sample N-50, Copper Substrate, 300 Volts Max.

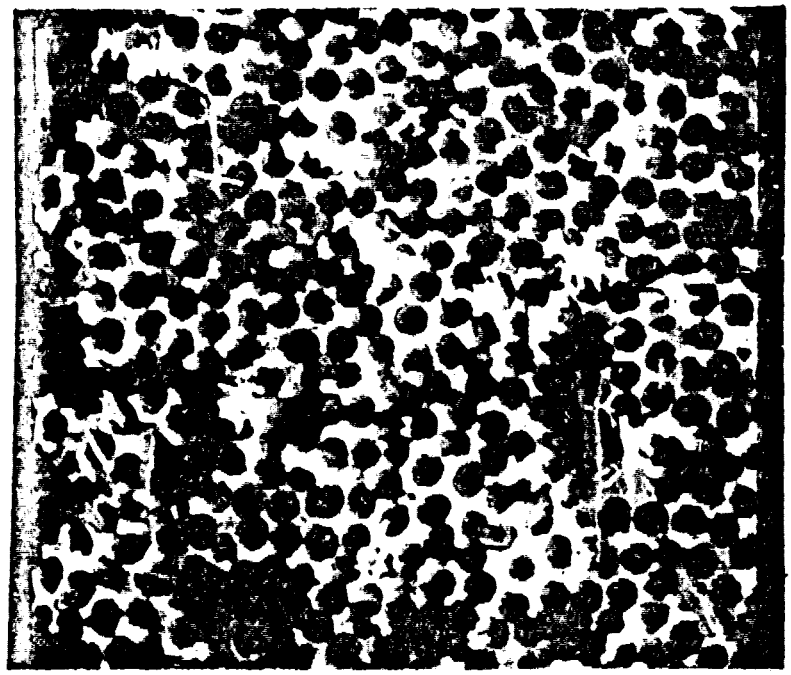

Pores of Sample N55, 0.4 micron diameter.
(10,000X)

Channels of Sample N56.
(3,000X)

Figure 5. Kapton Substrates ~300 Volts Max.

TABLE III

SAMPLES DELIVERED

Run	Substrate	Thickness		Comments	Quality
		Oxide (μ)	Total (μ)		
N-30	Aluminum	25-50	66	Poor	--
N-33	Aluminum	20-40	71	Do ion milling	Fair
N-34	Aluminum	35-70	80	Poor	--
N-35	Aluminum	25-50	70	Poor	--
N-36	Aluminum	25-35	85	Do ion milling	Fair
N41(P.E.)R	"	18	82	Do ion milling	Fair
N41(P.E.)2	"	18	82	Do ion milling	Fair
N-42	Aluminum	--	--	Poor	--
N-44	Aluminum	140-145	292	Poor	--
N-45	Stainless steel	36	94	Poor	--
N-46	Copper	36 max.	38	Do ion milling	Good
N-48	Teflon	10 max.	43	Do ion milling	Good
N-49	Copper	13-14	51	Do ion milling	Good
N-50	Copper	36	41	Do ion milling	Good
N-52	Copper	12	38	Do ion milling; oxide may be too thin.	Good
N-55	Kapton	28	39	Do ion milling	Good
N-56	Kapton	46	56	Do ion milling	Good
N-57	Teflon	--	Thick	Poor	--
N-58	Teflon	--	Thick	Poor	--

Thus, the estimated direct labor and materials costs for manufacturing the oxide masks is estimated at $4 to $6 per square foot.

4.0 DISCUSSION AND CONCLUSIONS

During this program, 58 samples were anodized. Nineteen samples on 5 different substrates were delivered to NASA-Lewis. Of these, 11 are worthy of being ion milled as indicated in Table III. Of these 11, 4 are on aluminum, 4 are on copper, 2 are on Kapton, and 1 is on Teflon. The stainless would probably have worked well if more specimens had been available to examine.

In general, the channels of the oxide fabricated from the vapor deposited aluminum on copper and Kapton were straight (parallel to each other, perpendicular to the surface, minimum wall roughness) and superior to those fabricated on the Teflon, and on the metallurgically worked aluminum metal with its residual strains and grain growth. In all probability, the Teflon would work as well if the vapor deposition process were refined to take into account Teflon's relative ease of thermal deformation.

It is possible to produce an integral oxide-substrate structure with no or minimal intervening residual aluminum. To do this consistently, the procedures used in this exploratory program need refinement.

For the samples fabricated at 600 volts, the pore diameters were 0.4 to 0.6 micron, with center-to-center spacing of 0.7 to 0.8 micron. For the samples fabricated at 300 volts, the pore diameters were typically 0.3 micron with center-to-center spacings averaging about 0.4 micron.

The pore enlargement done on sample N-41 resulted in pore diameters as large as 0.9 micron.

Until ion milling is done on the samples, it is not known what adjustments to the oxide mask would be needed. Hopefully, a mask thinner than many of these samples could be used.

At present it appears that the oxide masks can be made with straight channels and with appropriate pore diameters.

The estimated direct labor and materials costs to prepare an oxide mask from an aluminum vapor deposition coating of 25 microns is anticipated to be about $4 to $6 per square foot, provided the vapor deposition is done in a cont[illegible] wire fed 12 KW unit using an intermetallic composite [illegible] for the aluminum.

APPENDIX I

REVIEW OF POROUS OXIDE FORMATION ON ALUMINUM

REVIEW OF POROUS OXIDE FORMATION ON ALUMINUM

1.0 Introduction

To prepare a channel structured aluminum oxide of particular dimensions, the interrelationships of anodizing potential, current density, electrolyte type and concentration, bath temperature, and agitation must be understood and the proper combinations optimized. The mechanisms of oxide and pore growth and charge transport should also be understood. To a reasonable degree, the relationships of these variables are empirically known, but the detailed mechanism of oxide and pore growth is not well understood, although some important breakthroughs have been made. The purpose of this review is to acquaint the reader with the state-of-the-art of anodic oxidation of aluminum.

Aluminum can be electrochemically oxidized to form either one of the two distinct structures of oxide coating: a thin (generally $<1\mu$), continuous, nonporous oxide, or a thicker (Diggle et al estimated a maximum of $\sim 1000\mu$)[1] porous oxide which has a thin nonporous layer adjacent to the aluminum metal. The electrolyte used in the anodizing cell when aluminum is oxidized determines whether or not the oxide will be porous. If aluminum oxide is insoluble in the electrolyte, the thin, nonporous coating will result. Diggle et al state that such is the case with aqueous neutral boric acid, ammonium borate or tartrate, citric, malic and glycolic acid solutions and ammonium tetraborate in ethylene glycol.[1]

With electrolytes that can dissolve the oxide, the porous or channel structured oxide is formed. The most efficient electrolytes for this purpose are sulfuric, oxalic, chromic, and phosphoric acids along with mixtures of these acids with each other or the previously mentioned ones. The emphasis of this review is on porous oxide formation.

The following diagram of a porous aluminum oxide showing the nonporous layer or barrier-layer next to the metal, the cell and pore diameters, cell wall thickness, and radii of the pore and pore base will aid further discussion.

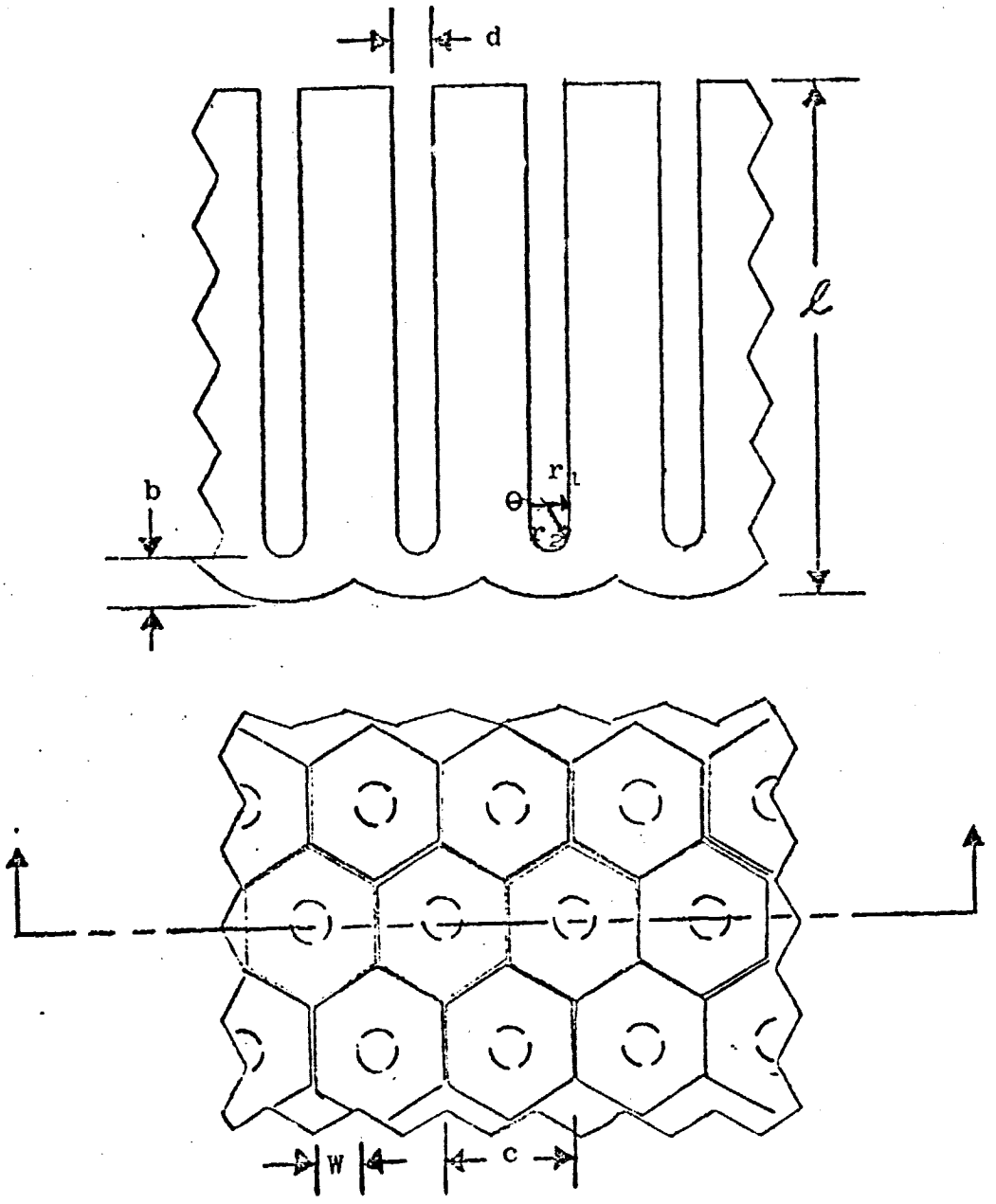

Figure 6

POROUS ALUMINUM OXIDE GEOMETRY. Showing the oxide thickness or channel length ℓ, pore diameter d, barrier layer thickness b, cell center-to-center spacing c, wall thickness W, pore radius r_1, pore base radius r_2, θ is discussed on pp. 32-33.

2.0 Relationships of Anodizing Variables

General relationships between current density, voltage, temperature, and electrolyte concentration for aluminum anodizing can be summarized as follows. To maintain constant current density with all other variables remaining constant, the necessary applied voltage* must be increased with time. At constant applied voltage, with all other variables remaining unchanged, the current density decreases with time.

The following schematics in Fig. 7 demonstrate the effect of temperature or concentration changes with constant voltage or constant current anodizing.

Increased electrolyte agitation will increase current density. Thus, for a constant voltage process, current density will increase and for a constant current density process, the voltage needed will decrease.

Oxide thickness is proportional to coulombs (current x time) passed.

3.0 Morphology of Oxide

With these general relationships in mind, a more detailed examination of how these variables influence the morphology of the oxide can be undertaken. An increase in voltage will produce an increase in barrier-layer thickness, cell and pore diameter. Keller et al[4] demonstrated that cell size increases approximately 20Å/V, and Hunter and Fowle[5,6] showed that barrier-layer thickness increases approximately 11Å/V, minor variations being due to different electrolytes used. Work in this laboratory with 0.3-2.0% oxalic acid at temperatures from zero to 25°C shows the cell size to increase 22Å/V over a voltage range of 0-600V. Formerly, Keller et al[4] theorized that cell size and cell wall thickness increased with potential, but that pore size remained constant. With

---

* In reasonably conductive solutions which are generally employed for anodizing, about 99% of the applied potential is effectively across the oxide, the remainder being lost in ohmic drops across the solution and junctions. Furthermore, little error is introduced by using the value of the applied potential in calculating the electric field in the oxide film. Thus, the applied Maxwell electric field is equal to the applied voltage divided by the thickness of the oxide.

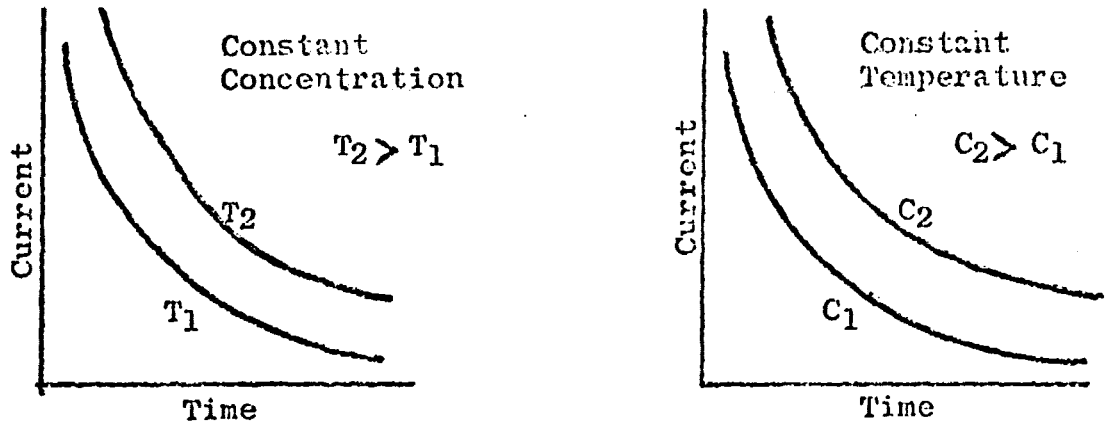

Constant Current

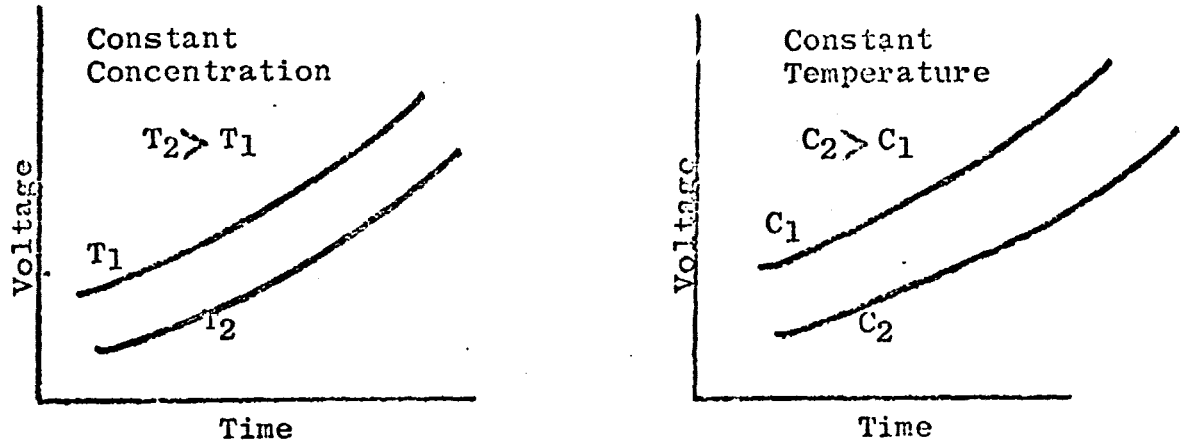

Figure 7

RELATIONSHIP OF EXPERIMENTAL VARIABLES

electron microscopy, O'Sullivan and Wood[2] showed that pore size is directly proportional to voltage. Over a limited potential range of 80-120 V, they showed that anodizing in 0.4 M phosphoric acid at 25°C for 1 hour produced pore diameters of 12.9Å/V. Also, the cell wall thickness was always 0.71 of the barrier-layer thickness. From limited data at higher anodizing voltages, Lasser et al[7] proved that pore diameter did increase with voltage. At 150 V in 1.5% oxalic acid at 4°C, the pore diameter was 910Å; at 500 V in 0.75% oxalic acid at 0°C, the pore diameter was 1790Å. Work in this laboratory with 0.5% oxalic acid at 0°C shows the pore diameter to increase by 4.5Å/V over the 0 to 600 V range.

Since cell size increases with voltage, the number of cells per unit area of aluminum surface or pore density will decrease. The amount of open channel space or porosity is a function of pore diameter and pore density. With an increase in voltage, pore diameters increase but pore densities decrease. Under some conditions these two phenomena can exactly balance each other and porosity is independent of voltage. O'Sullivan and Wood[2] have concluded that phosphoric acid coatings formed at 80-120 volts have a 21% porosity which is invariant. However, when using data of Lasser et al[7] at higher voltages, it is found that the open volume is not a constant. At 500 V the porosity is 47% of that at 150V. This follows from some arithmetic on their data: the pore and cell diameters are 910Å and 4,170Å at 150 V and 1,970Å and 12,222Å at 500 V. Additional work is needed in this area to clarify the conditions which control porosity.

Changes in temperature and electrolyte concentration will also influence barrier-layer thickness and pore and cell diameters. Temperature changes will be considered first. With constant current density, since an increase in temperature will decrease voltage, barrier-layer thickness and pore and cell diameters will also decrease. With a constant voltage process, an increase in temperature would not be expected to have much influence on barrier-layer thickness and cell and pore diameters because their sizes change with a voltage change. Some data are available for both of these cases. For constant current density anodizing at $100 Am^{-2}$ in 0.4 M phosphoric acid, an increase in temperature from 20 to 30°C decreased the barrier-layer thickness from 1400 to 1000Å, the pore diameter from 1600 to 1120Å, and the cell diameter from 3470 to 2870Å. For a

constant 80 V process in the same solution, a temperature increase from 20 to 30°C produced virtually no change in cell diameter, an increase in pore diameter from 920 to 1220Å, and a small decrease in barrier-layer thickness from 910 to 820Å.[2]

Electrolyte concentration changes will now be discussed. With constant current density and temperature, as the electrolyte concentration is increased, voltage decreases and so must the barrier-layer thickness and cell and pore diameters. But, for a constant voltage process, a concentration increase would not be expected to influence barrier-layer thickness, pore and cell diameters very much. O'Sullivan and Wood[2] showed, for a constant 100Am^{-2} at 25°C anodizing, that as the phosphoric acid concentration was increased from 0.4 to 2.5 M, voltage fell to the point that the barrier-layer thickness decreased from 1050 to 130Å, the pore diameter from 1600 to 570Å, and the cell diameter from 3500 to 940Å. For a constant 80 V process at 25°C, the same concentration increase produced no change in pore diameter, a small decrease from 2430 to 2080Å in cell diameter, and a small decrease from 880 to 670Å in barrier-layer thickness.

No discussion of oxide morphology would be complete without a description of channel uniformity. Here the literature is lacking, but recent examination in this laboratory of oxides formed under various conditions with the scanning electron microscope have given some insight. The electrolyte used seems to play a major role. The straightest and most uniform channels are formed in a dilute oxalic acid solution. Channels formed in chromic acid are twisted while those formed in phosphoric acid are frequently non-parallel, wavy and branching, especially if the coating has been burned.

O'Sullivan and Wood[2] showed by electron microscopy of stripped thin films that nonuniform barrier-layer thickening eventually became the sides of the pores. Pore growth was evident very early in the process. A typical run might be a half to a few hours in length and they saw pore growth within 80 seconds when a constant current density of 50Am^{-2} was applied to an aluminum electrode in 0.4 M ($\sim$4%) phosphoric acid at 25°C. The main pores and cells appeared to develop most rapidly along the metal subgrain boundaries. Herenquel and LeLong[3] reported that the oxide grows preferentially on the 111 plane and minimally along the 100 plane.

4.0 Theory of Pore Growth

Various theories of pore formation have been suggested with later ones often incorporating parts of earlier ones. The following explanation of pore growth, by O'Sullivan and Wood[2], is the most consistent with all available experimental data and is also internally consistent.

The dissolution of aluminum oxide to form the pores is felt to be field assisted and to a large extent field controlled, rather than a simple chemical dissolution whose rate is determined by the solubility of aluminum oxide in the given electrolyte and the temperature produced by the current. The postulate of field assisted dissolution helps explain facts like the following:

(1) O'Sullivan and Wood[2] stated that films grown at $500Am^{-2}$ thicken about 5 times faster than those grown at $100Am^{-2}$ in the same solution, but the barrier layer thickness in each case is essentially the same.

(2) Hunter and Fowle[6] calculated the dissolution rate of oxide during anodizing at $200Am^{-2}$ in 1.5 M sulfuric acid at 21°C to be 3725Å/min. Chemical dissolution under these conditions is only 0.84Å/min.

(3) O'Sullivan and Wood[2] and Lasser et al[7] demonstrated that when the anodizing voltage is increased, pore diameter is also increased.

(4) Over a limited range of 80-120 V, O'Sullivan and Wood[2] found a constant angle of Cos^{-1} 0.71 between the pore base radius and pore radius (see Fig. 6).

Pore growth can be viewed as follows. The average field within the barrier layer determines the growth of the film, while the stronger field at the base of the pore assists the dissolution. Since at the base of the pore, dissolution is assisted more than film growth, the pore can propagate. Because the barrier layer at the pore base is thinner than elsewhere, the current density at the pore base is greater than elsewhere. Other thin areas can produce pores only if they can compete with the established pores for current. If the dissolution proceeds such as to widen the pores, the field strength at the pore base will lessen and film growth

will overtake dissolution. When the pore becomes more narrow, the field at the pore base will be increased and will accelerate dissolution of the oxide. This type of mechanism would tend to produce pores of a size and geometry characteristic of the anodizing voltage and other variables. Over the limited 80-120 volt range, the angle θ between the pore radius and pore base radius of curvature was found to be $\cos^{-1} 0.71$, or approximately 49°.[2] At higher voltages, Lasser et al[7] reported cells and pores which seem consistent with the voltages.

If the dissolution of aluminum oxide is viewed as necessitating the cleavage of the Al-O bond, any weakening of this bond would enhance dissolution. Near the pore base, the field would tend to pull O^{2-} ions into the oxide and repel Al^{3+} ions into the solution.

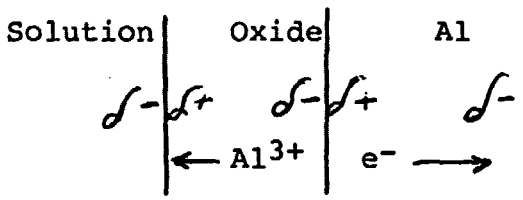

Figure 8. Dissolution

This repelling of the Al^{3+} would work to weaken the Al-O bond in the oxide. Along with the field effect, the electrolyte itself can aid dissolution by hydrogen bonding. O'Sullivan and Wood[2] felt that the O^{2-}, OH^- or H_3O^+ ions trapped in the lattice would aid hydrogen bonding more than those migrating. The following data are in agreement with the idea of hydrogen bonding. Murphy[3] showed pore density to increase with an increase in the log of a quantity proportional to the acid dissociation constant for the series 4% phosphoric, 3% chromic, 2% oxalic, and 15% sulfuric acids.

The above data and theory of pore growth can be explained and summarized as follows. At constant voltage, the barrier-layer thickness remains essentially unchanged with time. This means oxide growth and dissolution at the pore base are occurring at the same rate. The channels must transport anions to the pore base and cations to the solution bulk. As the channels

grow in length, this transport becomes more difficult and the current flowing in the channels, which is caused by this ion transport, decreases with a resultant decrease in dissolution. As the dissolution current decreases so must the current within the oxide and aluminum metal which propagates the pores. Hence, at constant voltage the current density decreases.

With a constant current density system, a similar argument applies. In order to keep the same current flowing through the electrolyte in the channels and in the oxide and metal, as the channels grow in length a stronger field (more voltage) is continually needed to enable the ions in solutions to overcome resistance in the channels due to the physical geometry of the channels and concentration gradients. Hence, at constant current density, increased voltages must be applied.

With constant voltage anodizing, the oxide growth and dissolution are closer to steady-state than with constant current density anodizing and the response in these processes to temperature and electrolyte changes can be more accurately predicted and controlled with constant voltage than with constant current anodizing.

At constant voltage, an increase in temperature will facilitate ion transport and the current density will increase. Not much change is expected in barrier-layer thickness and pore and cell diameters, but the combined effect of higher temperature and current density does increase oxide dissolution at the pore base. With a thinner barrier layer, the pore diameter must increase in order to hold the pore geometry constant (see Fig. 6 and the significance of Θ). With constant current density anodizing, an increase in temperature facilitates ion transport and decreases the voltage requirement. With a lower voltage, barrier-layer thickness decreases as does cell and pore diameters since these are directly proportional to voltage. The relationship between barrier-layer and cell wall thickness remains constant. The barrier-layer thickness would be expected to decrease slightly because of possible increased dissolution. However, the O'Sullivan and Wood data show it to increase slightly.[2]

At constant voltage and temperature, an increase in electrolyte concentration increases current density. Here, again, barrier-layer thickness, cell and pore diameters would not be expected to be much influenced, but the increased current densities decrease the barrier-layer thickness because of increased dissolution. With a thinner barrier layer, the cell walls become thinner. At constant current density and temperature, an electrolyte concentration increase facilitates ion transport and hence decreased voltage, which in turn decreases barrier layer and pore and cell diameters.

5.0 Oxide Composition and Ion Transport

The above theory and discussion leaves unanswered questions about which aluminum oxide is formed during anodizing and which ions carry the charge within the oxide and the corresponding transport mechanism which is responsible for oxide growth. These are the questions which still need researching to a large degree although some small amount of insight is available.

Franklin[9] reported three types of oxide on films formed in a boric acid-borax electrolyte: 1) a hydrated oxide near the electrolyte side of the film, 2) irregular patches of γ-Al_2O_3, and 3) an amorphous oxide comprising the majority of the film. Similar results were reported by Trillat and Tertain[10] for films formed in 20% aqueous sulfuric acid: an outer layer consisting of a mixture of boehmite, AlO(OH), and crystalline γ-Al_2O_3 and an inner layer of amorphous Al_2O_3. More recent infrared work by Dorsey[25] suggested that the barrier layer is a hydrogen bonded trihydrate with aluminum existing in both the divalent and trivalent oxidation states. In the porous section of the oxide, Dorsey suggests the Al = O bond exists. He has further evidence that the barrier layer is composed of higher molecular weight polymers than the porous layer.

A number of experiments have been performed to determine which ions are mobile in the oxide, and the most recent consensus is that both anions and cations are mobile.[12-17] The mobile cations would be aluminum and, according to Young,[11] their oxidation state would not necessarily be equal to three, or they would have a range of oxidation states. Hoar and Mott[18] feel the mobile anions are OH^-; Davies et al[19] and Brock and Wood[20] feel the mobile anions are O^{2-}; and Hoar et al feel the mobile anions are oxyanions from the acid.

Various equations and models have been proposed to describe ion transport in the oxide. The reader is referred to References 1, 11 and 22 for a thorough discussion of them. Briefly, the Cabrera-Mott theory is directed at very thin films (20-100Å) and hypotheses that the transfer of an ion across the metal-oxide interface is the rate-determining step. The ionic current density i_+ is expressed as

$$i_+ = nvq \exp[-(W-qaE)/kT]$$

where n is the surface density of mobile ions at the metal, v is the vibration frequency of a surface metal ion, W is the activation energy, q is the charge on the mobile ion, a is the activation distance. E is the electric field, k is the Boltzman constant, and T is the absolute temperature. (Typical values at room temperature, for Al^{3+} with $q = 3$, $a = 1Å$, and $E = 6 \times 10^6$ Vcm^{-1}, are $qaE = 0.3$ eV, $W = 1_eV$ and $V = 10^{14}$ sec^{-1}.) Several inadequacies of this theory stem from $(ae/_{kT})$ not being exactly temperature dependent, a being too large, and log i_+ vs E being slightly nonlinear.

In the Verwey theory, the movement of the ions through the oxide are considered to be the rate determining step. The equation here is similar to that above and suffers from the same limitations.

In the Dewald theory, the movement of the ion across the metal-oxide interface and through the oxide are both considered rate determining. In addition, allowance has been made for a space charge effect. This theory accounts for the experimental data for thick films better than the Verwey theory, but it along with the other two cannot account for transient behavior unless the additional hypothesis of the interstitial ion concentration varying sluggishly with the electric field is introduced. All of these theories use a Maxwell electric field and some evidence[23,24] is available to suggest using a Lorentz

$$\left(E_L = \frac{E_M}{3}(\varepsilon + 2) \quad \text{where} \quad \varepsilon = \text{oxide dielectric constant}\right)$$

field instead. Furthermore, all of these theories have one additional limitation -- they are based on a crystalline model and the oxide is largely amorphous.

From this latter discussion about the details of porous aluminum oxide growth and the earlier discussions about porous aluminum oxide growth in general, it can be seen that a significant body of data is available and can be empirically but not quantitatively explained.